RSC Advances

ROYAL SOCIETY OF CHEMISTRY

www.rsc.org/advances

RSC Advances

Method

A theoretical study on the hetero-Diels-Alder reaction of phosphorous substituted diaza- and oxaza-alkenes with olefins derivatives

Received 00th January 20xx,
Received 00th January 20xx,
Accepted 00th January 20xx

DOI: 10.1039/x0xx00000x

www.rsc.org/

M. Haghdadi*, A. Abaszade, L. Abadian, N. Nab and H. Ghasemnejad Bosra

*mhaghdadi2@gmail.com

The reactivity, regio- and stereo-selectivity of the hetero-Diels-Alder reaction of 1,2-diaza- and 1,2-oxaza-1,3-butadiene derivatives with some olefins has been investigated using density functional theory (DFT) based reactivity indices and activation energy calculations at theB3LYP/cc-pVDZ level of theory. Four reactive pathways associated with *ortho* and *meta* regio- and *endo* and *exo* stereo-selectivity have been explored and characterized. Analysis of the results indicates that these reactions take place via an asynchronous concerted bond-formation process with a polar character. All of studied processes predicted *ortho* regioselectivity and in the majority of them the *endo* approach appeared to be energetically favored, in agreement with experimental finding. Phosphonyl and phosphinyl groups increased the reactivity of the 1,2-oxaza-1,3-butadienes, shown by decreasing activation energies. DFT-based reactivity indices correctly explain the polar nature of these cycloaddition reactions.

Introduction

Since 1928, there are many papers concerning synthetic, mechanistic and theoretical aspects of Diels-Alder reactions, with about half of these appearing in the last decade [1]. When one or more heteroatoms are present in the diene and/or dienophile framework, the cycloaddition is termed a hetero Diels-Alder (HDA) reaction. Such reactions present an elegant and versatile procedure in the preparation of non-carbogenic systems [2]. In particular, the process enables the synthesis of biologically important nitrogen- and oxygen- containing heterocycles, hitherto inaccessible or difficult to achieve using standard methods [3]. Nitroso-alkenes and aza-alkenes, used as heterodienes in cycloaddition reactions with a range of nucleophiles, alkenes and heterocycles, have proved to be valuable tools for the synthetic organic chemist.

A common feature of both nitrosoalkenes and aza-alkenes is that they possess a highly electrophilic carbon center (C_4 in conjugated nitroso- and aza-alkenes, see Figure 1) that allows cycloaddition reactions, particularly those with nucleophilic olefins, to take place under very mild conditions. Such reactions have provided routes to a variety of novel heterocyclic structures which have proved to be very useful targets, not only because of their biological and pharmacological properties, but also due to their versatile use as synthetic intermediates for the synthesis of amino acids, pyroles, prolines, indoles, pyrazines and aza-sugars derivatives, to name but a few [4-15].

Theoretical calculations have shown that 1,2-diazabutadiene, as an aza-alkene, is a more efficient diene than 1- and 2-azabutadienes for the formation of heterocycles by aza-Diels-Alder processes [16]. Some examples of 1,2-oxaza-alkenes (**1**) and 1,2-diaza-alkenes (**2**) substituted on the terminal carbon (C_4) (R"=Me, Br, Cl, COR, CO_2R, $CONR_2$) [17-20] and the terminal nitrogen (N_1) (R=Me, Ar, ArSO, COR, CO_2R, $CONR_2$), [17,19] Figure 1, have been reported, as well as some limited information on the behavior of heterodienes containing phosphorus substituents on C_4 [21-22].

Insert Figure 1

The phosphorus substituents are important biological functions [23]. The molecular modifications involving the introduction of organo phosphorus functionalities in simple synthons could be very interesting from a synthetic point of view because they can be useful substrates for the preparation of biologically active compounds.

In this context, recent reports describe the generation of phosphinyl (R"=$PO(Ph)_2$) and phosphonyl (R"=$PO(OEt)_2$) nitroso-alkenes [24-26] and 1,2-diaza-alkenes, [22, 27-29] and investigate the cycloaddition processes of these heterodienes [30] with olefins to generate phosphorus substituted heterocycles. The mechanism of HDA reactions of these phosphorus substituted nitroso-alkenes and 1,2-diaza-alkenes with olefins has not been fully explored. For this reason, we

[a] *Department of Chemistry, Islamic Azad University, P.O. box 755, Babol branch, Babol, Iran. mhaghdadi2@gmail.com*

† Electronic Supplementary Information (ESI) available: [details of any supplementary information available should be included here]. See DOI: 10.1039/x0xx00000x

wish to propose a mechanism for these HDA reactions, suggested by our computational work.

We present herein the results of a density functional theory (DFT) study on the HDA reactions between two families of heterodienes, 4-phosphorated 1,2-diaza-1,3-butadiene (**3**) and 4-phosphorated or 4-carboxylic acid 1,2-oxaza-1,3-butadiene (**4**), with a series of dienophiles, 2,3-dihydrofuran (**5a**), cyclopentadiene (**5b**), styrene (**10**) and vinyl ethyl ether (**15**), which were reported by Palacios and de los Santos [22,26]. Our aim is to contribute to better understanding of the influence of phosphoryl substituents and heteroatoms on the reactivity of these HDA reactions and the origins of the kinetic outcomes, and also to shed some light on the mechanistic details of these reactions. Then, we address a theoretical study to investigate these reactions based on DFT-based reactivity indices.

Computational methods

The ubiquitous B3LYP [31] hybrid functional has been the workhorse of quantum chemical studies on organic molecule for years [32]. It is well known that B3LYP could describe interactions in the DA reactions. Recently, some functional, such as the MPWB1K, [33] have been proposed to investigate reaction energies, barrier heights and intermediates for the Diels-Alder reactions. For a comprehensive comparison of geometries, we were prompted to optimize all species of the aforementioned HDA reactions using both B3LYP and MPWB1K exchange-correlation functional. The cc-pVDZ basis set was used for full optimization with the B3LYP method and single point energy evaluation with the MPWB1K method. The electronic energies were corrected with ZPE at the B3LYP/cc-pVDZ level. All calculations were performed using Gaussian09 [34]. The values of the relative energies, ΔE, have been calculated on the basis of total energies of stationary points. Relative enthalpies, ΔH, entropies, ΔS, and free Gibbs energies, ΔG, were calculated with the standard statistical thermodynamics at 298.15 k [35].

The electronic structures of stationary points were analyzed by the natural bond orbital (NBO) method [36]. Global reactivity indices were estimated according to the equations proposed by Parr and Yang [37]. The global electrophilicity index, ω, which measures the stabilization in energy when the system acquires an additional electronical charge N from the environment has been given by the following simple expression [38]

$$\omega=\mu^2/2\eta \quad (1)$$

where μ is the electronic chemical potential and η is the chemical hardness. Both μ and η may be evaluated in terms of the one-electron energies of the frontier molecular orbitals HOMO and LUMO, ε_H and ε_L, [37] using:

$$\mu = \varepsilon_H + \varepsilon_L /2 \quad (2)$$

$$\eta=\varepsilon_L-\varepsilon_H \quad (3)$$

Also, Domingo introduced an empirical (relative) nucleophilicity index, N, [39] based on the HOMO energies obtained within the Kohn Sham scheme, [40] defined as:

$$N=\varepsilon_H(NU)-\varepsilon_H(TCE) \quad (4)$$

Nucleophilicity is referenced to tetracyanoethylene (TCE), because this has the lowest HOMO energy in a large series of molecules already investigated in the context of polar cycloadditions. This choice allows us to conveniently handle a nucleophilicity scale of positive values. Recently, Domingo proposed two new electrophilic, P_k^+ and nucleophilic, P_k^- Parr functions [41], which were obtained through analysis of the Mulliken atomic spin density of the radical anion and cation by single-point energy calculations over the optimized neutral geometries using the unrestricted UB3LYP formalism for radical species. The local electrophilicity indices, ω_k [41], and the local nucleophilicity indices, N_k [41], were calculated using the following expressions:

$$\omega_k = \omega P_k^+ \quad (5)$$

$$N_k = N P_k^- \quad (6)$$

Where P_k^+ and P_k^- are the electrophilic and nucleophilic Parr functions [41], respectively. Therefore, one can easily find the ω_{max} and N_{max}, which are associated with the more electrophilic and most nucleophilic centers in a molecule, respectively, and correspond to the centers with the highest electron density developed along the CT process [41].

The transition states were verified by analysis of the internal reaction coordinates (IRC) for both forward and reverse directions [42].

Results and discussion

First, the energetic aspects and geometrical parameters of the transition states (TSs) and their electronic structures in terms of bond orders and natural charges will be analyzed. Then, DFT analysis of the global reactivity indices of the reactants involved in these HDA reactions will be performed.

To obtain a quantitative estimate of the conformational energies in such systems, conformational analysis of pyridazine and oxazine rings were carried out on all the stationary points at the B3LYP/cc-pVDZ level, which showed that the distorted boat conformers are more stable than the chair ones. This result is in agreement with experimental data [22,26].

Study of the potential energy surface of the polar HDA reaction of 4-phosphinyl-1,2-diaza-1,3-butadiene (3a) and 4-phosphonyl-1,2-diaza-1, 3-butadiene (3b) with 2,3-dihydrofuran (5a) and cyclopentadiene (5b).

Due to the asymmetry of the reagents, the HDA reactions between 1,2-diaza-1,3-butadienes **3a** and **3b** with cycloolefines **5a** and **5b** can take place along two stereoisomeric reactive pathways, *endo* and *exo*, and two regioisomeric pathways, *ortho* and *meta*. Therefore these cycloaddition reactions can proceed *via* four reaction pathways, involving the transition states TS1, TS2, TS3 and TS4, giving four corresponding cycloadducts, (CAs), **6**, **7**, **8** and **9**. (Scheme 1)

Insert Scheme 1

The stationary points associated with the HDA reaction between **3a** and **3b** with **5a** and **5b** are presented in Scheme 1, together with the atom numbering, while the relative energies are summarized in Table 1.

Insert Table 1

From Table 1, we can see that in the HDA reaction of **3+5**, the energy barriers for all processes in *ortho* pathways are lower than in *meta* ones, and the *endo* TSs are more stable than the *exo* ones except in the cycloaddition reaction of **3b** with **5a**, where the *ortho-exo* pathway is more stable than others. In some processes, the cycloadducts formed from the *exo* approach in *ortho* pathways are more stable than those formed from the *endo* approach (**3a**+**5a** and **3a**+**5b**) and in others the stability are almost the same. This competition between a kinetically favored reaction pathway and a thermodynamically favored product is responsible for the mixture of stereoisomers that are observed experimentally [22].

Also, the values of the Gibbs free energies, enthalpies, and entropies associated with the four reactive pathways are summarized in Tables 1 and S1. Analysis of the activation enthalpy and Gibbs free energy show a preference for the *ortho* pathways, in agreement with the computed activation energy. Moreover, all the reactions progressed exothermically with large ΔH values (Table S1). According to Hammond's postulate, the TSs should then be closer to the reactants.

With Comparing the HDA reactions of **3a** and **3b** with **5a** and **5b** gives the following conclusions:

I) The activation barriers for the HDA reactions of **3a** and **3b** with 1, 2-dihydrofuran, **5a**, in the more favorable pathways (*ortho*) are lower in energy than those for the HDA reactions of **3a** and **3b** with cyclopentadiene **5b**.

II) The stereoselectivity increased in the HDA reactions of **3a** with **5a** and **5b**, which is likely to be due to the steric effect of phenyl group on phosphorous. (The differences of energy between *the endo* and *exo* pathways are about 5 kcalmol^{-1}).

III) The large difference in activation energies of the HDA reaction of **3a** with **5a**, $\Delta\Delta E^{\#}$> 5 kcalmol^{-1}, gives a reaction that is under full kinetic control, with the most of product being **6aa**. In the reactions of **3b** with **5a**, $\Delta\Delta E^{\#}$<1.5 kcalmol^{-1}, and of **3b** with **5b**, $\Delta\Delta E^{\#}$<2 kcalmol^{-1}, a mixture of the CAs, **6** and **7** are expected. The experimental results confirmed these data (see footnote of Table 1).

IV) All of these HDA reactions are strongly exothermic, with ΔE_r between -31.25 and -44.62 kcalmol^{-1}, and so they can be considered irreversible.

The geometries of the TSs involved in these HDA reactions are presented in Figures 2 and S1. The extent of bond formation along a reaction pathway is providing by the concept of bond order (BO) [43]. This theoretical tool has been used to study the molecular mechanism of chemical reactions and to evaluate the asynchronicity for the formation processes. The BO values of N_1-C_6 and C_4-C_5 forming bonds along the *ortho* approach modes are between 0.28 to 0.34 and 0.18 to 0.20 at TS1 and 0.30 to 0.33 and 0.15 to 0.21 at TS2, respectively. Also, along the *meta* approach modes the BO values of the N_1-C_5 and C_4-C_6 forming bonds are between 0.29 to 0.35 and 0.13 to 0.24 at TS3 and between 0.26 to 0.32 and 0.1 to 0.27 at TS4, respectively. These data indicate that while the N-C forming bond is very advanced, the C-C bond is not being bonded in these TSs. Also, the most favorable *ortho* TSs is more asynchronous than the *meta* ones.

The extent of the asynchronicity also, can be measured from the difference between the distances of the bonds that are being formed in the reaction, that is, Δr_{ortho}=d(C_4-C_5)-d(N_1-C_6) and Δr_{meta}=d(C_4-C_6)-d(N_1-C_5). For example, for the TSs of **3a+5a** HDA reaction, the Δr values are 0.13 (TS1aa), 0.41 (TS2aa), 0.16 (TS3aa) and 0.29 (TS4aa). Thus the endo TSs are more asynchronous than exo ones.

Insert Figure 2

The natural population analysis (NPA) allows us to evaluate the charge transfer (CT) along these HDA reactions [44]. The natural atomic charges at the TSs were shared between the heterodiene **3** and dienophile **5**. At the TSs associated with the HDA reaction between **3a** and **5a**, the CT that fluxes from **5a** to **3a** is about 0.29 e at TS1 and TS2, and about 0.32 e at TS3 and TS6. While at the TSs associated with the HDA reaction of **3b** and **5a**, the CT fluxes from **3b** to **5a** (within the range of 0.23 e to 0.30 e) at TS1 and TS2 and are about 0.23 e at TS3 and TS4.

As can be seen in Figures 2 and S1, in the HDA reactions of **3a** and **3b** with **5b**, the CT at the TSs are a slightly lower in compared to HDA reactions of **3a** and **3b** with **5a** and also, the values of CT predicting a slightly more polar character for the *endo* pathways to *exo* ones.

In order to compare the B3LYP energy results with MPWB1K ones, the stationary points were optimized, as a single point calculation at MPWB1K/cc-pVDZ using the optimized geometry at B3LYP/cc-pVDZ level of theory. The MPWB1K relative energies are given in Tables S2 and S3. A comparison of the relative energies indicates that while the MPWB1K activation energies are lower than those of the B3LYP ones, the exothermic is increased as a consequence of a lower stabilization of reagents than TSs and cycloadducts. However inclusion of diffuse functions does not modify the selectivities.

Study on the potential energy surface of HDA reaction of 4-phosphinyl-1, 2-diaza-1, 3-butadiene (3a) and 4-phosphonyl-1, 2-diaza-1, 3-butadiene (3b) with styrene (10).

An analysis of the stationary points in the HDA reactions between **3a** and **3b** with styrene **10** indicates that they can take place through four reactive pathways, *ortho, meta, endo* and *exo* possibilities. Thus, four TSs, TS5, TS6, TS7 and TS8, and four CAs, **11**, **12**, **13** and **14**, have been found and characterized for each HDA reactions (Scheme 3). The stationary points associated with these reactions are presented in Scheme 2, and the relative energies are summarized in Table 1. The geometries of the TSs are presented in Figures 2 and S1.

Insert Scheme 2

As can be seen in Table 1, for the HDA reactions **3a** and **3b** with **10** the activation energies in the *ortho* pathways are more favorable than the *meta* ones and *endo* approach modes of *ortho* are more stable than *exo* ones, which leading to the formation of the *ortho* cycloadducts **11** and **12**. This can explain the kinetically favoured formation of cycloadducts **11a** and **11b** as compared to the formation of other cycloadducts, in agreement with the experimental results [22].

The presence of phenyl group on phosphorous caused the high regioselectivity for the HDA reaction of **3a** with **10**, $\Delta\Delta E^{\#}$ >7

kcalmol^{-1}, while the mixture of **11a** and **12a** are expected for existence of the low stereoselectivity $\Delta\Delta E^{\#}$<2.5 kcalmol^{-1}.

The BO values of N_1-C_6 and C_4-C_5 forming bond along the *ortho* pathways are in range of 0.38 to 0.2 at TS5 and 0.4 to 0.2 at TS6, respectively, while along *meta* pathways the BO values of the N_1-C_5 and C_4-C_6 forming bonds are in range of 0.43 to 0.21 at TS7 and 0.30 to 0.23 at TS8, respectively (Figures 2 and 1S).

In the HDA reaction of **3a** with **10**, the CT increased during the *ortho* pathway and it fluxes from **10** to **3a,** 0.2e for TS5a and TS6a, and 0.18e for TS7a and TS8a. While, in the HDA reaction of **3b** with **10** the CT of TSs doesn't change through the *ortho* and *meta* pathways (0.21e). These CT values show a polar character for these processes.

Study on the potential energy surface of HDA reaction of 4-phosphinyl-1,2-oxaza-1, 3-butadiene (4a), 4-phosphonyl- 1,2-oxaza-1, 3-butadiene (4b) and 1,2-oxaza-1, 3-butadiene-4-carboxylic acid (4c) with vinyl ethyl ether (15).

Analogously, we next investigated the stereo- and regioselectivity in the HDA reaction of nitroso-alkenes **4a, 4b** and **4c** with vinyl ethyl ether, **15,** which for each pathways (*ortho* and *meta*), two possible approaches of vinyl ethyl ether **15** to nitroso-alkene **4**, *exo* and *endo*, were located and characterized (Scheme 3). Therefore, four CAs, **16**, **17, 18** and **19** were considered and the activation and relative energies are summarized in Table 1. The geometries of TSs are shown in Figures 3 and S2.

Insert Scheme 3

The results of calculations indicated completely *ortho* regioselectivity, as all *ortho* transition structures lie lower in energy than the corresponding *meta* ones (Table 1). In the HDA reaction of 1,2-oxaza-1, 3-butadiene **4a**, while the TS11a is about 10 kcalmol-1 higher in energy than TS9a, high regioselectivity, (in clear agreement with the results of experiment [26]) the stereoselectivity as the energy differences of *endo*- and *exo*-*ortho*, is low, <1 kcalmol^{-1}. Thus the both pathways (*endo* and *exo*) are predicted to be competitive, which the experimental results showed a mixture of *endo/exo* CAs in a 50:50 ratio [26]. The formation of CAs is strongly exothermic, between -30.29 and -41.10 kcalmol^{-1}, then these reactions can be considered irreversible.

On the other hand, in the HDA reaction of **4b** (R=PO(OEt)$_2$) with **15**, TS10b in the *ortho-exo* pathway has the lowest energy, and stereoisomer **17b** with the high stability could be the result expected under kinetic and thermodynamic control conditions (Table 1). From Table 1, a comparison of the activation energies of these HDA reactions indicates that, the stereoselectivity of the HDA reaction of **4b** increased which is in agreement with the experimental results, a mixture of *endo/exo* CAs with 25:75 ratio was obtained [26].

Next, the HDA reaction of nitroso-alkene **4c** with **15** was studied (Scheme 3). The activation and relative energies associated with the four reactive pathways are displayed in Table 1. The energy results indicated that this reaction has highly *ortho* regioselectivity and *exo* stereoselectivity, as the most favorable *ortho* TS, TS10c, is 15.74 kcalmol^{-1} below *meta* ones and is4.4 kcalmol^{-1} lower in energy than *endo* ones, which is in good agreement with the experimental observations. These energy values clearly indicated that the presence of CO_2Et group in the nitroso-alkene (**4c**) increased the stereoselectivity. With considering the experimental and theoretical results for these HDA reactions studied, the regioselectivity and stereoselectivity are in agreement under kinetic control.

Insert Figure 2

The geometries of TSs are shown in Figures 3 and S2. The BO values of these TSs indicated that C_4-C_5 forming bonds along the *ortho* pathways are in the range of 0.1 to 0.24 at TS9 and 0.11 to 0.25 at TS10 and for O_1-C_6 forming bond the BO values change between 0.31 to 0.55 at TS9 and 0.29 to 0.57 at TS10. The BO values of O_1-C_5 forming bonds along *meta* pathways are around 0.3 to 0.39 at TS11 and for C4-C6 forming bond change in range of 0.21 to 0.28 at TS12. These results indicated that the most favorable *ortho* TSs are more asynchronous than the *meta* ones and the O-C bond formation is more advanced than the C-C bond formation. Also, the CT values in Figure 3 and S2, predicting a more polar character for these HDA reactions.

By comparison the activation energy of HDA reactions of 1,2-diaza- and 1,2-oxaza-1,3-butadiene derivatives, **3** and **4** (see Table 1), it is clear that in the HDA reactions **4** with dienophiles ,**15**, the energy barriers decreased but the stability of CAs increased and also, a high regioselectivity was seen in these HDA reactions.

Moreover, the experimental results showed that the CAs, **6** and **16** can epimerized to **7** and **17**, respectively, then we analyzed the calculated Gibbs free energies for these processes (Scheme 4). The differences of Gibbs free energies for compounds **6ba** and 1**6b** are about 1.83 kcalmol^{-1} and 3.37 kcalmol^{-1} more stable than compounds **7ba** and **17b** (Scheme 4), and **7aa** and **17a** are about 5.15 kcalmol^{-1} and 1.61 kcalmol^{-1} more stable than **6aa** and **16b**, respectively, which these results are in accord with the easy epimerization of these compounds.

Insert Scheme 4

With Considering the FMO approach, (Table 2), the energy values of HOMO and LUMO for all reactants indicated that these HDA reactions undergo inverse electron demand cycloadditions.

Insert Table 2

DFT-based reactivity indices

Studies devoted to cycloaddition reactions [45] have shown that the analysis of the global and local the reactivity indices defined within the context of conceptual DFT [46], is a powerful tool to understand the reactivity in cycloadditions. The global indices, namely, electronic chemical potential μ, chemical hardness η, global electrophilicity ω and global nucleophilicity N, for the reagents involved in these HDA reactions are given in Table 2.

As can be seen from Table 2, the electronic chemical potential of heterodienes (**3a**, μ=-4.54 eV, **3b**, μ=-4.57 eV, **4a**, μ=-4.66 eV, **4b**, μ=-4.73 eV and **4c**, μ=-4.82 eV) are lower than dienophiles (**5a**, μ=-3.29 eV ,**5b**, μ=-3.24 eV ,**10**, μ=-3.64 eV and **15**, μ=-3.40 eV), indicating that the charge transfer (CT) for

these cycloaddition reactions will take place from dienophile frameworks towards heterodienes.

The dienophiles **5a, 5b** and **15** present nucleophilicity, N, index of 3.50 eV (**5a**) , 3.21 eV (**5b**) and 3.13 eV (**15**) and electrophilicity, ω, index of 1.14 eV , 0.96 eV and 1.10 eV respectively. According to the absolute scale of nucleophilicity and electrophilicity, these compounds may be classified as strong nucleophiles [47], and as marginal electrophiles [48].

Also, styrene **10** has a significant electrophilicity value, ω=1.30 eV, being classified as a moderate electrophile, where as it presents a high nucleophilicity value, N=2.94 eV, allowing for its classification as a strong nucleophile. On the other hand, heterodienes of 1,2-diaza-1,3-butadienes **3a** and **3b** and 1,2-oxaza-1,3-butadienes **4a, 4b** and **4c** have a high electrophilicity values, ω=2.41 eV, 2.44 eV, 3.48 eV, 3.52 eV and 3.79 eV, respectively, making it possible to classify these species as strong electrophiles on the electrophility scale. The electrophilicity of **4a, 4b** and **4c** is higher than that of 1,2-diaza-1,3-butadiens **3a** and **3b**, which indicates that the presence of the nitroso group increases the electrophilicity. Consequently, the strong electrophilic character of 1,2-oxaza-1,3-butadienes **4a, 4b** and **4c** and the strong nucleophilic character of vinyl ethyl ether **15** account for the very low activation energy computed for these HDA reactions.

The relationship between the difference in electrophilicity for the heterodiene/dienophile pair, Δω , and the static polarity may be a useful tool to describe the electronic pattern expected for the TSs involved in the HDA reaction describing low polar (Δω small) or high polar (Δω big) mechanism [49]. The high Δω between **3a** and **5a**, 1.27 eV, 1.45 eV for **3a+5b**, 1.30 eV for **3b+5a**, 1.48 eV for **3b+5b**, 1.113 eV for **3a+10** and 1.14 eV for **3b+10** show a high polar character of these HDA reactions. Note that for the HDA reactions of 1,2-oxaz -1,3-butadiens **4a, 4b** and **4c** with vinyl ethyl ether, **15**, Δω increased to 2.38 eV for **4a+15** , 2.42 eV for **4b+15** and 2.69 eV for **4c+15**.

These results show the HDA reactions of **4** with **15** are more polar than **3** with **5** and **10**. These analyses are in clear agreement with the high charge transfer found at TSs. The charge transfer pattern for the HDA processes may be estimated using the values of electronic chemical potential and chemical hardness, for reactants. Thus by enhancement in charge transfer of HDA reactions of 1,2-oxaza-1,3- butadienes (**4a**-**4c**) to 1,2-diaza-1,3-butadienes (**3a** and **3b**), the chemical potential difference is increased, Δμ=2.38 eV for **4a/15**, Δμ=2.42 for **4b/15** and Δμ=2.69 for **4c/15** interaction. In addition a simultaneous decreasing in the chemical hardness of 3.12 eV (**4a**), 3.18 eV (**4b**) and 3.06 eV (**4c**) were observed, which is with the low resistance to the charge transfer.

Along a polar reaction involving the participation of non-symmetric reagents, the most favourable reactive pathway is that involving the initial two-center interaction between the most electrophilic centers of the electrophile and the most nucleophilic center of the nucleophile [39].

Insert Table 3

Recently, Domingo et al. have proposed the electrophilic P_k^+ and nucleophilic P_k^- Parr functions, derived from the changes of the electron density from the nucleophile to the electrophile, as powerful tools in the study of the local reactivity in polar processes [41]. Hence, in order to characterise the most nucleophilic and the most electrophilic centers of the species involved in these HDA reactions, the nucleophilic P_k^- Parr functions of dienophiles **5**, **10** and **15** and the electrophilic P_k^+ Parr functions of heterodienes **3** and **4** were analysed. The parr functions computed based on the Mulliken atomic spin density analysis and the local electrophilicity indices (ω_k) and local nucleophilicity indices (N_k) for N_1, O_1, C_4, C_5 and C_6 atoms of the heterodienes **3a, 3b, 4a, 4b** and **4c**, and the dienophiles **5a, 5b, 10** and **15** are computed and given in Table 3.

Analysis of the nucleophilic P_k^- Parr functions at 2,3-dihydrofuran **5a** indicates that the C_6 atom is the most nucleophilic center of this species, presenting the maximum value, P_k^-= 0.48 (see Scheme 1 for atomic numbering). At this carbon atom, the value of the local nucleophilicity N_k index is N_{C6} = 1.66 eV. Note that the local nucleophilicity N_k index at the C_5 carbon in **5a** presents a very low value, N_{C5} = 0.31 eV. On the other hand, the electrophilic P_k^+ Parr functions of 1,2-diaza-butadiene **3a** indicates that the nitrogen N_1 atom is *ca.* twice as electrophilically activated, P_k^+= 0.35, as the terminal C_4 carbon, P_k^+=0.15. The corresponding local electrophilicity, ω_k, values are ω_{N1} = 0.85 eV and ω_{C4} = 0.37 eV, respectively. Therefore, the most favourable electrophile-nucleophile interaction along the nucleophilic attack of **5a** on **3a** will take place between the most nucleophilic center of 2, 3-dihydrofuran **5a**, the C_6 atom, and the most electrophilic center of 1,2-diaza-butadiene **3a**, the N_1 atom leading to the formation of CAs, **6** and **7** which is in agreement with the experimental observation [22]. The same results obtained for the HDA reactions **3a+5b**, **3b+5a** and **3b** with **5b.** Moreover, in the HDA reaction of **3a** and **3b** with **10**, the most favorable two-center interaction take place between N_1 atom of **3** with C_6 atom of **10** and C_4 atom of **3** with C_5 atom of **10**, leading to the formation of the **11** and **12** stereoisomers, which is in agreement with the experimental finding [22]. These results are in agreement with the most favorable cycloadducts, **6, 7, 11** and **12**, which show that the N_1-C_6 bond formation is more advanced than the C_4-C_5 one.

In the HDA reactions of **4a, 4b** and **4c** with **15** , the most favorable two-center interaction take place between the most nucleophilic center of **15**, (P_k^- *and* N_{C5}), the C_5 atom, and the most electrophilic center of 1,2-oxaza-1,3-butadienes **4a, 4b** and **4c** , (P_k^+ *and* N_{O1}) the O_1 atom. These analyses are in clear agreement with the geometrical and electronic structures of the most favorable pathways, in HDA reactions of **3** and **4**, which show that the N_1-C_6 and O_1-C_6 bond formation is more advanced than the C_4-C_5 one.

Conclusion

4-phosphinyl and 4-phosphonyl- 1,2-diaza- and 1,2-oxaza-1,3-butadienes **3** and **4** with some olefins **5, 10** and **15** were studied using the DFT method at the B3LYP/cc-pVDZ and MPWB1K/cc-pVDZ levels. The computational studies of the molecular mechanism indicated that the conjugated 1,2-diaza and 1,2-oxaza-alkenes participate as heterodiene through the nitroso and diaza groups, toward cyclic or acyclic olefins, such as 2,3-dihydrofuran (**5a**), cyclopentadiene (**5b**), styrene (**10**)

and vinyl ethyl ether (**15**) to afford the corresponding cycloadducts.

These HDA reactions take place through a one-step mechanism, with complete *ortho* regioselectivity, *via* asynchronous concerted mechanism through *endo* or *exo* transition states. The MPWB1K calculations predict a similar *ortho* regioselectivity that obtained with B3LYP calculation and appear lower activation energies than the B3TYP ones.

The global indices allow to anticipate the polar character of the reaction as well the shift of the CT along the cycloaddition process. Analysis of the global indices indicates that the presence of nitroso group at the 1,2-oxaza-butadiene increased the electrophilic activation and polarity of these HDA reactions. Moreover, an analysis of the parr functions on these reactions allows us to explain the most favorable two –center interaction between the highest nucleophilic and electrophilic sites of the reagents which is responsible for the regioselectivity observed in these polar cycloaddition.

Finally, the results obtained in this work allow us to conclude that the activation energy calculations and DFT-based reactivity indices clearly predict the regio- and stereochemistry of the isolated cycloadducts.

Acknowledgements

The authors wish to acknowledge Dr Louise S. Price, University college London, UK, for reading the manuscript and providing valuable suggestions.

References

1. F. Finguelli and A. Tatichhi, *The Diels-Alder reaction: Selected practical methods,* Eds. John Wiley & Sons, Ltd, U.K, 2002.
2. D.L. Boger, *Tetrahedron,* 1983, **39**, 2869; D.L. Boger, *J. Heterocycl. Chem.,* 1996, **33**, 1519.
3. D.L. Boger, *Chem. Rev*., 1986, **86**, 781.
4. E.M. Stocking, and R.M. Williams, *Angew. Chem. Int. Ed.,* 2003, **42**, 3078.
5. K.C. Nicolau, M. Nevalainen, B.S. Safina, M. Zak and S. Bulat, *Angew. Chem. Int. Ed.,* 2002, **41**, 1941.
6. O.A. Attanasi, and P. Filippone, *Synlett .,* 1997, 1128.
7. O.A. Attanasi, L. De Crescentini, G. Favi, P. Filippone, G. Giorgi, F. Mantenilli, and S. Santeusanio, *J. Org. Chem.,* 2003, **68**, 1947.
8. M. Avalos, R. Babiano, F.R. Clemente, P. Cintas, R. Gordillo, J.L. Jiménez and J.C. Palacios, *J. Org. Chem*., 2000, **65**, 8251. ; M. Avalos, R. Babiano, Cintas, F.R. Clemente, R. Gordillo, J.L. Jiménez, and J.C. Palacios, *J. Org. Chem.,* 2002**, 67**, 2241.
9. O.A. Attanasi, L. De Crescentini, P. Filippone, F. Fringelli, F. Mantenilli, M. Metteucci, O. Piermatti, and F. Pizzo, *Helv. Chim. Acta.,* 2001, **84**, 513.
10. P. Kafarski, and B. Lejezak, *Phosphorus Sulfur,* 1991, **63**, 193.
11. F.Palacios, E. Herrán, and G. Rubiales, *J. Org. Chem.,* 2002, **67**, 2131.
12. F. Palacios, D. Aparicio, and J.M. de los Santos, *Tetrahedron,* 1999, **55**, 13767.
13. F. Palacios, A.M. Ochoa de Retana J.I. Gil, and R. López de Munain, *Org. Lett.,* 2002, **4**, 2405. ; F. Palacios, D. Aparicio, A.M. Ochoa de Retana, J. M.de los Santos, J.I. Gil, and Alonso, J.M. *J. Org. Chem.,* 2002, **67**, 7283.
14. F. Palacios, D. Aparicio, and J. Vicario, *Eur. J. Org. Chem.,* 2002, 4131.
15. F. Palacios, D. Aparicio, De los Santos, J.M. and J. Vicario, *Tetrahedron,* 2001, **57**, 1961.
16. R.K. Boeckman Jr, P. Ge, and J.E. Reed, *Org. Lett.,* 2001, **3**, 3647.
17. O.A. Attanasi, L. De Crescentini, P. Filippone, F. Mantinelli, and S. Santeusanio, *ARKIVOC*, 2002, 274.
18. M. Avalos, R. Babiano, P. Cintas, F.R. Clemente, R. Gordillo, J.L. Jimènez, and J.C. Palacios, *J.Org. Chem.* 2002, **67**, 2241.
19. J.G. Schantl, T.L. Gilchrist, A. Lemos, and T.G. Roberts. *Tetrahedron*, 1991, **47**, 5615.
20. J.G. Schantl, and P. Nadenik, *Synlet*, 1998, 786.
21. F. Palacios, D. Aparicio, Y. López, and J.M. De los Santos, *Tetrahedron Lett*. 2004, **45,** 4345.
22. F. Palacios, D. Aparicio, Y. López, J.M. De los Santos, and C. Alonso, *Eur. J. org. chem.,* 2005, 1142.
23. P. Kafarski, and B. Lejeza *Phosphorus Sulfur,* 1991, **63**, 193.
24. J.M. De los Santos, R. Ignacio, D. Aparicio, and F. palacios, *J. Org. Chem.,* 2007, **72**, 5202.
25. J.M. De los Santos, R. Ignacio, D. Aparicio, F. palacios, and J.M. Ezpeleta, *J. Org. Chem.,* 2009, **74**, 3444.
26. J.M. De los Santos, M. Jesús, R. Ignacio, Z.E. Sbai, D. Aparic, and F. Palacios, *J. Org. Chem.,* 2014, **79**, 7607.
27. Palacios, F. Ochoa de Retana, A.M. Gil, J.I. and López de Munain, R. *Org. Lett.,* 2002, **4**, 2405.
28. F. Palacios, A.M. Ochoa de Retana, and J. Pagalday, *Eur. J. Org. Chem.,* 2003, 913.
29. F. Palacios, D. Aparicio, and J. Vicario, *Eur. J. Org. Chem.,* 2002, 4131.
30. J.M. De los Santos, R. Ignacio, G. Rubiales, D. Aparicio, and F. Palacios, *J. Org. Chem.,* 2011, **76**, 6715.
31. A.D. Becke, *Phys. Rev .A.* 1988, **38**, 3098; C. Lee, W. Yang, and R.G. Parr, *Phys. Rev .B.* 1988, **37**, 785.
32. L. Simon, and J.M. Goodman, *Org. Biomol. Chem.,* 2011, **9**, 684.
33. L.R. Domingo, M.J. Aurell, and P. Pérez, *Tetrahedron,* 2014, **70**, 4519.
34. M.J. Frisch, G.W. Trucks, H.B. Schlegel, G.E. Scuseria, M.A. Robb, J.R. Cheeseman, V.G. Zakrzewski, J.A.Jr. Montgomery, R.E. Start-mann, J.C. Burant, S. Daprich, J.M. Millam, A.D. Daniels, K.N. Kudin, M.C. Strain, O. Farkas, J. Tomasi, V. Barone, M. Cossi, R. Cammi, B. Mennucci, C. Pomelli, C. Adamo, S. Clifford, J. Ochterski, G.A. Petersson, Y. Ayala, Q.C. Ui, K. Morokuma, D.K. Malick, A.D. Rubuck, K. Raghavachari, J.B. Foresman, J. Cioslowski, J.-V. Oritz, B.B. Stefanov, G. Liu, A. Liashenko, P. Piskorz, I. Komaromi, R. Comperts, R.L. Martin, D.J. Fox, T. Keith, M.A. Al-Laham, C.-Y. Peng, A. Nanayakkara, C. Gonzalez, M. Challa-combe, M.W. Gill, B. Johnson, W. Chen, M.-W. Wong, J.L. Andres, C. Gonzalez, M. Head-Gordon, E. S. Replogle, and J.A. Pople, *Gaussian 09 revision A.* 2009, Gaussian, Pittsburgh.
35. W.J. Hehre, L.Radom, P.v.R. Schleyer, and J.A. Pople, *Ab initio molecular orbital theory*. Wiley: New York, 1986.

36. A.E. Reed, R.B. Weinstock, and F. Weinhold, *J. Chem. Phys.,* 1985, **83**, 735.
37. R.G. Parr, and W. Yang, *Density functional theory of atoms and molecules.* Oxford: New York, 1989, 16.; R.G. Parr, and R.C. Pearson, J. Am. Chem. Soc., 1983, **105**, 7512.
38. R.G. Parr, L.V. Szentpaly, and S. Liu, *J. Am. Chem. Soc., 1999,* **121**, 1922.
39. L.R. Domingo, and P. Pérez, *J. Org. Chem.,* 2008, **73**, 4615. ; L.R. Domingo and P. Pérez, *Org. Biomol. Chem.*, 2011, **9**, 7168.
40. W. Kohn and L.J. Sham, *Phys. Rev. A*, 1965, **140**, 1133.
41. L.R. Domingo, P. Pérez, and J.A. Saez, *RSC Adv.,* 2013, **3**, 7520.; L.R. Domingo, P. Pérez, and J.A. Saez, *RSC Adv.,* 2013, **3**, 1486.
42. C. Gonzalez , and H.B. Schlegel, *J. Phys. Chem.,* 1990, **94** , 5523.
43. K.B. Wiberg, *Tetrahedron,* 1968, **24**, 1083.
44. L.R. Domingo, E. Chamorro, and P. Pérez, *Lett. Org. Chem*., 2010, **7**, 432.
45. R.G. Parr, and W. Yang, *Annu. Rev. Phys. Chem*., 1995, **46 ,** 701; H. Chermette, *J. Comput. Chem.,* 1999, **20** , 129.
46. D.H. Ess, G.O. Jones, and K.N. Houk, *Adv. Synth. Catal.,* 2006, **348**, 2337.
47. P. Jaramillo, L.R. Domingo, E. Chamorro, and P. Pérez, *J. Mol. Struct.:THEOCHEM*, 2008**, 865**, 68.
48. L.R. Domingo, M.J. Aurell, P. Pérez, and R. Contreras, *Tetrahedron*, 2002, **58**, 4417.
49. H. Chemouri, and S.M. Mekellecche, *Int, J. Quantum Chem .,* 2012, **112**, 2294.

Table 1- The calculated activation energies ($\Delta E^{\#}$/kcalmol^{-1}), activation Gibbs free energies ($\Delta G^{\#}$/ kalmol^{-1}) and reaction energies (ΔEr/kcalmol^{-1}) of the HDA reactions between 1,2-diaza-1,3-butadiene and 1,2-oxaza-1,3-butadienes derivatives (**3** and **4**) with some olefins (**5**, **10** and **15**) at the B3LYP/cc-pVDZ level of theory (For a full comparison of energies see supporting information).

Species	TS	$\Delta E^{\#}$	$\Delta G^{\#}$	ΔEr
3a+5a→6aa	**TS1aa**	10.86	25.47	-36.64[a]
3a+5a→7aa	**TS2aa**	16.27	30.77	-41.54[a]
3a+5a→8aa	**TS3aa**	16.00	30.05	-41.98
3a+5a→9aa	**TS4aa**	19.52	34.39	-41.48
3b+5a→6ba	**TS1ba**	12.24	26.33	-37.87[a]
3b+5a→7ba	**TS2ba**	11.11	24.34	-37.79[a]
3b+5a→8ba	**TS3ba**	13.55	27.17	-44.62
3b+5a→9ba	**TS4ba**	12.92	27.35	-37.78
3a+5b→6ab	**TS1ab**	12.99	27.67	-31.25[a]
3a+5b→7ab	**TS2ab**	17.57	32.75	-36.71[a]
3a+5b→8ab	**TS3ab**	13.97	26.68	-31.48
3a+5b→9ab	**TS4ab**	18.97	34.28	-36.15
3b+5b→6bb	**TS1bb**	12.31	25.28	-39.76
3b+5b→7bb	**TS2bb**	14.12	27.59	-39.68
3b+5b→8bb	**TS3bb**	13.03	25.86	-39.56
3b+5b→9bb	**TS4bb**	15.48	28.82	-39.06
3a+10→11a	**TS5a**	13.36	28.61	-35.04
3a+10→12a	**TS6a**	15.26	30.51	-37.08
3a+10→13a	**TS7a**	20.27	35.83	-33.19
3a+10→14a	**TS8a**	24.47	40.35	-37.40
3b+10→11b	**TS5b**	11.97	26.49	-39.97
3b+10→12b	**TS6b**	12.69	26.60	-43.23
3b+10→13b	**TS7b**	13.47	26.76	-40.28
3b+10→14b	**TS8b**	16.56	30.87	-43.36
4a+15→16a	**TS9a**	7.90	24.03	-39.60[b]
4a+15→17a	**TS10a**	8.75	25.25	-41.10[b]
4a+15→18a	**TS11a**	18.31	34.98	-34.39
4a+15→19a	**TS12a**	23.30	40.48	-30.29
4b+15→16b	**TS9b**	8.02	22.89	-41.12[b]
4b+15→17b	**TS10b**	6.29	22.08	-44.87[b]
4b+15→18b	**TS11b**	22.23	37.98	-36.42
4b+15→19b	**TS12b**	21.00	37.34	-36.03
4c+15→16c	**TS9c**	11.41	26.36	-42.24[b]
4c+15→17c	**TS10c**	7.01	21.58	-43.48[b]
4c+15→18c	**TS11c**	19.62	34.22	-33.02
4c+15→19c	**TS12c**	22.75	37.46	-34.93

[a] The ratio of *endo* to *exo*-isomers in the experimental results were obtained for the HDA reactions of **3a+5a, 3b+5a** and **3a+5b**, 97:3, 28:72, and 69:31, respectively. [b] The ratio of *endo* to *exo*-isomers in the experimental results were obtained for the HDA reactions of **4a+15, 4b+15** and **4c+15 0** 50:50, 25:75 and 0:100, respectively.

Table 2- HOMO energies/au, LUMO energies/au, electronic chemical potential (μ/eV), chemical hardness (η/eV), global electrophilicity (ω/eV) and nucleophilicity (N/eV) for the reactants obtained at the B3LYP/cc-pVDZ level of theory.

Species	E_{HOMO}	E_{LUMO}	*μ*	*η*	*ω*	*N*
3a	-0.24610	-0.08881	-4.544	4.280	2.412	2.459
3b	-0.24688	-0.08951	-4.571	4.283	2.439	2.438
5a	-0.20797	-0.03330	-3.292	4.762	1.138	3.499
5b	-0.21849	-0.01891	-3.238	5.431	0.965	3.213
10	-0.22840	-0.03986	-3.646	5.129	1.296	2.941
4a	-0.22878	-0.11400	-4.653	3.120	3.480	2.931
4b	-0.23282	-0.11589	-4.734	3.181	3.522	2.825
4c	-0.23405	-0.12163	-4.816	3.058	3.792	2.781
15	-0.22145	-0.02882	-3.401	5.240	1.103	3.133

Table 3- The Parr functions (P_k^+/au), local electrophilicity indices (ω_k /eV) and local nucleophilicity indices (N_k/eV) at the reactive sites of the reactants calculated at the B3LYP/cc-pVDZ level of theory.

Species	*k*	P_k^+	P_k^-	ω_k	N_k
3a	N1	**0.348**	0.124	0.846	0.307
	C4	0.153	0.063	0.373	0.154
3b	N1	**0.351**	0.187	0.858	0.456
	C4	0.158	0.042	0.388	0.104
5a	C5	0.506	0.087	0.217	0.307
	C6	0.261	**0.475**	0.112	1.664
5b	C5	0.101	0.088	0.096	0.285
	C6	0.386	**0.454**	0.369	1.459
10	C5	0.044	0.010	0.057	0.029
	C6	0.395	**0.417**	0.513	1.227
4a	O1	**0.353**	0.341	1.186	1.034
	C4	0.013	0.209	0.727	0.038
4b	O1	**0.596**	0.364	1.284	1.680
	C4	0.081	0.227	0.801	0.228
4c	O1	**0.654**	0.337	1.287	1.818
	C4	0.122	0.186	0.710	0.339
15	C6	0.552	**0.414**	0.207	1.727
	C5	0.062	0.411	0.205	0.194

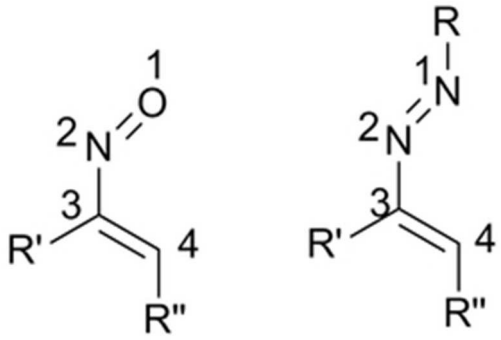

Figure 1-1,2-oxaza-1,3-butadiene (1) and 1,2-diaza-1, 3-butadiene (2) showing potential substitution sites.

21x14mm (300 x 300 DPI)

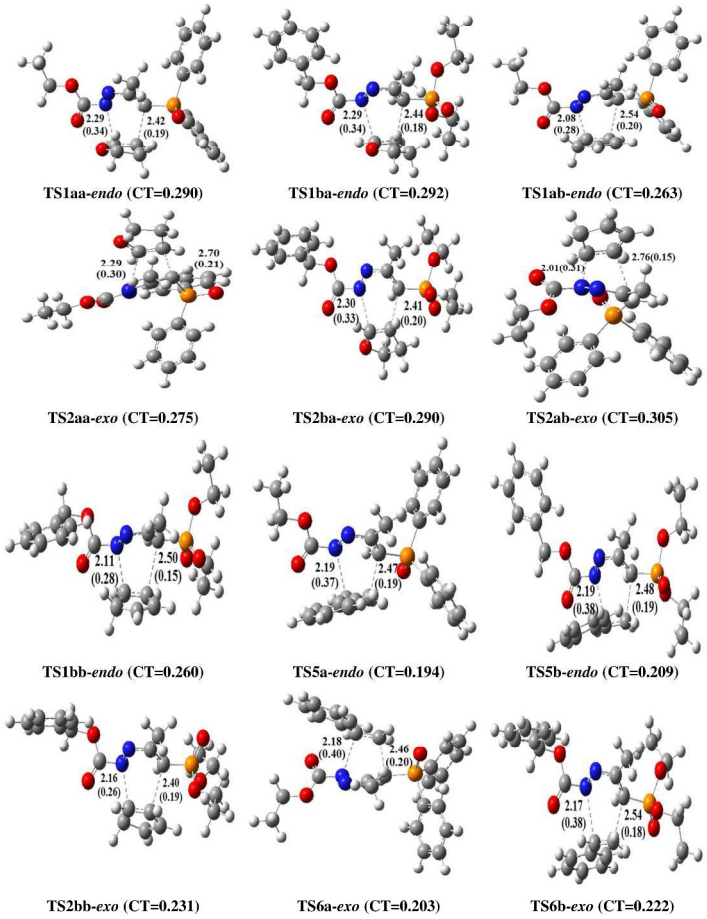

Figure 2- The geometry optimized transition states for ortho pathways of the HDA reactions between 1,2-diaza-1,3-butadiene derivatives (3a and 3b) and some olefines (5a and 5b) at the B3LYP/cc-pVDZ level of theory. Bond distances are given in Å, wiberg bond indices are given in parentheses and the natural charges (CT) of TSs are also given (For a full comparison of geometries see supporting information).

297x420mm (300 x 300 DPI)

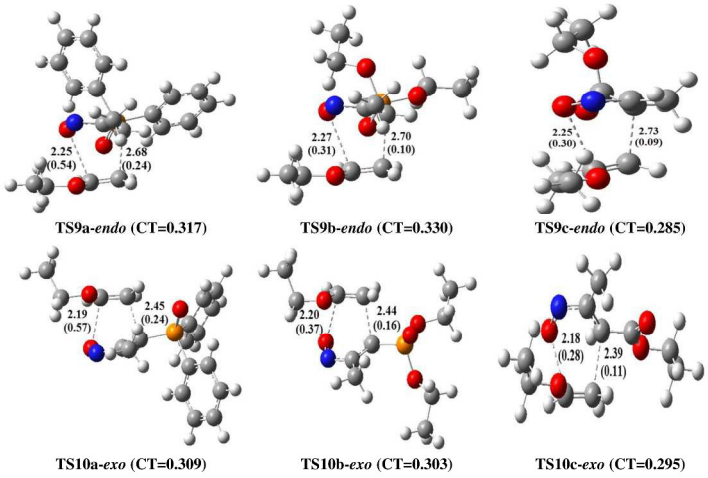

Figure 3- The geometry optimized transition states for ortho pathways of the HDA reactions between 1,2-oxaza-1,3-butadiene derivatives (4a and 4b) and vinyl ethyl ether (15) at the B3LYP/cc-pVDZ level of theory. Bond distances are given in Å, wiberg bond indices are given in parentheses and the natural charges (CT) of TSs are also given (For a full comparison of geometries see supporting information).

297x420mm (300 x 300 DPI)

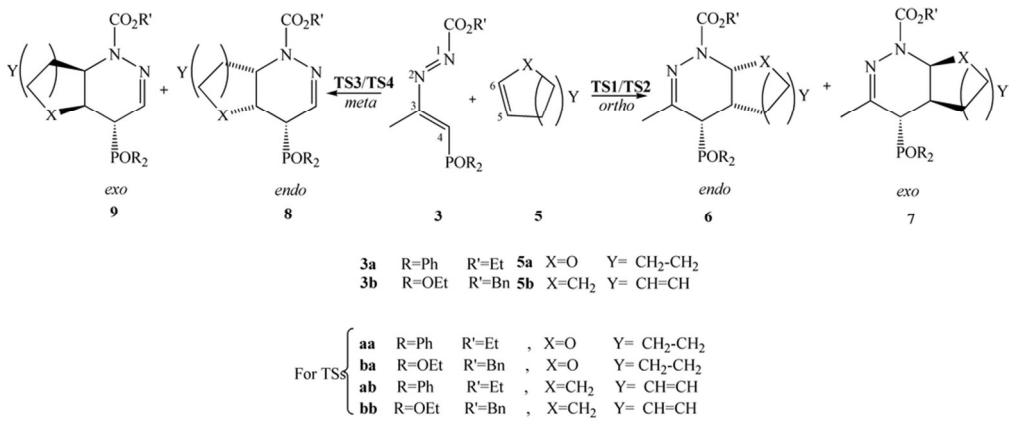

Scheme 1. ‖ ┼ The calculated possible reaction pathways for the HDA reaction of 1,2-diaza-1,3-butadiene derivatives (3) with some olefins (5) at the B3LYP/cc-pVDZ level of theory.‖ ┼

89x37mm (300 x 300 DPI)

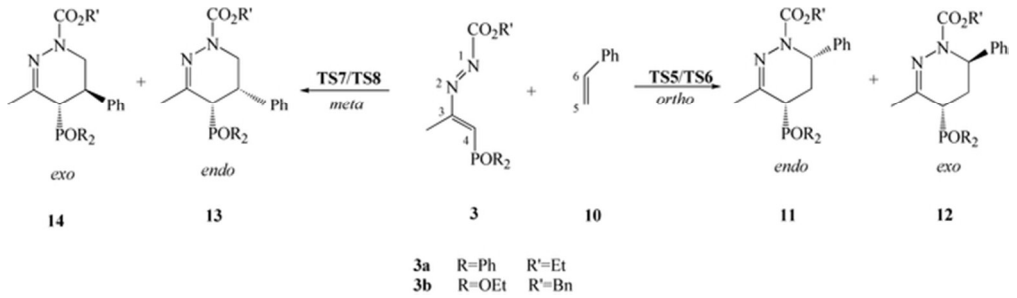

Scheme 2 ‼ ┼ The calculated possible reaction pathways for the HDA reaction of 1,2-oxaza-1,3-butadiene derivatives (4) with vinyl ethyl ether (15) at the B3LYP/cc-pVDZ level of theory.‼ ┼

58x16mm (300 x 300 DPI)

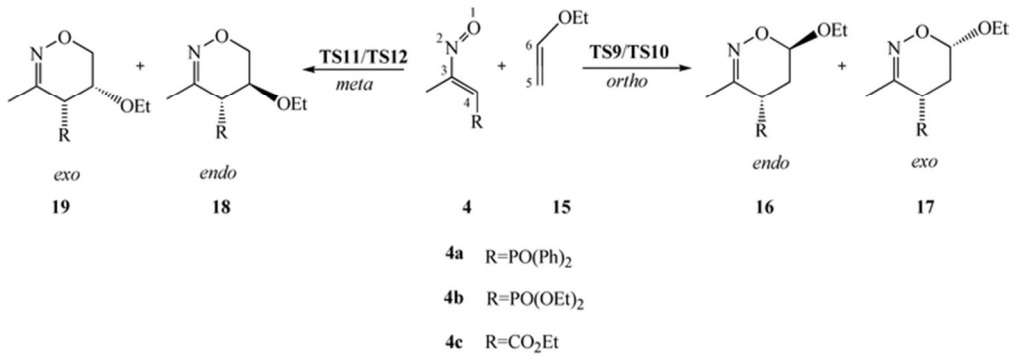

Scheme 3. ‼ ┼ The calculated possible reaction pathways for the HDA reaction of 1,2-oxaza-1,3-butadiene derivatives (4) with vinyl ethyl ether (15) at the B3LYP/cc-pVDZ level of theory.‼ ┼

65x22mm (300 x 300 DPI)

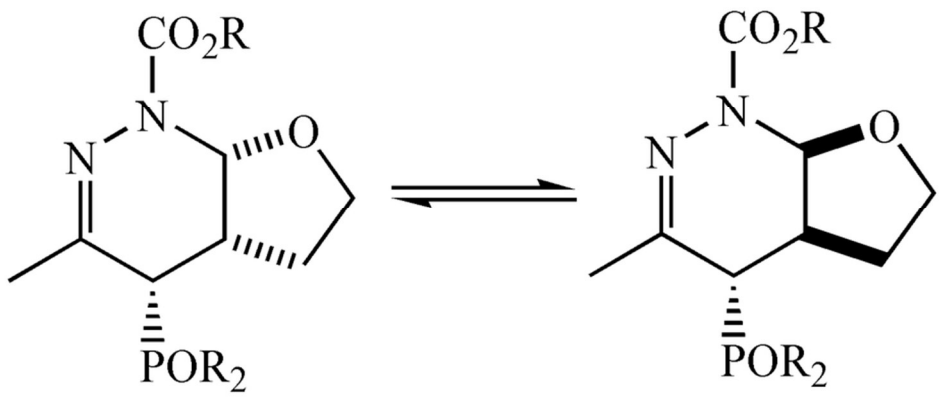

	ΔG (kcalmol^{-1})	
6aa	5.15	**7aa**
6ba	-1.83	**7ba**

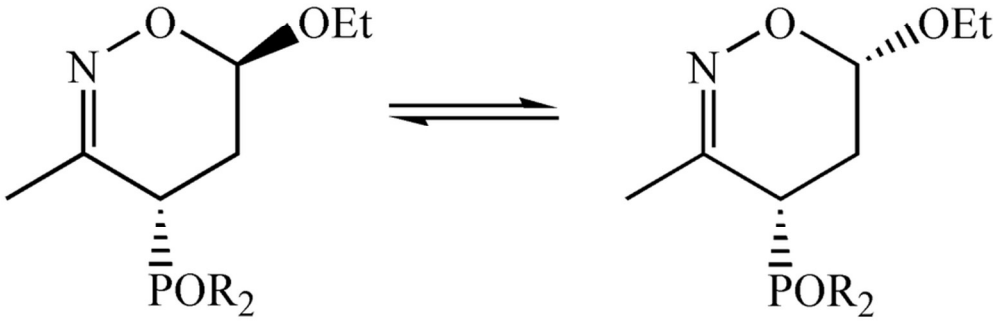

	Δ G (kcalmol^{-1})	
16a	1.61	**17a**
16b	-3.37	**17b**

Scheme 4. The calculated free energies for the conversion process of endo and exo stereoisomers at the ortho pathways.

82x99mm (300 x 300 DPI)

A theoretical study on the hetero-Diels-Alder reaction of phosphorous substituted diaza- and oxaza-alkenes with olefins derivatives

M. Haghdadi*, A. Abaszade, L. Abadian, N. Nab and H. Ghasemnejad Bosra

Department of Chemistry, Islamic Azad University, P.O. box 755, Babol branch, Babol, Iran

*mhaghdadi2@gmail.com

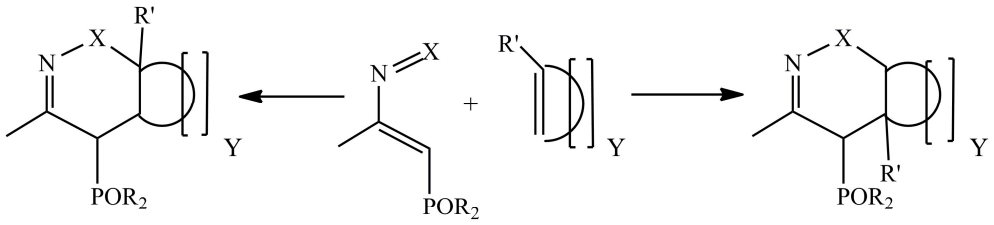

X=NCO_2Et or O Y=OCHCH, CH_2CHCH, H

DFT studied indicated that hetero-Diels-Alder reaction of 4-phosphinyl and 4-phosphonyl-1,2-diaza- and 1,2- oxaza-1,3-butadienes with some olefins take place *via* asynchronous concerted mechanism through *endo* or *exo* transition states.